Research Square

Preprints are preliminary reports that have not undergone peer review.
They should not be considered conclusive, used to inform clinical practice,
or referenced by the media as validated information.

# Strengthening effects of different alloying elements in CoNiCr-Bbased filler metals on brazed joints of single crystal superalloy DD6

**Wen-wen Li**
AVCC Beijing Institute of Aeronautical Materials: Aero Engine Corporation of China Beijing Institute of Aeronautical Materials

**Bo Chen**
AVCC Beijing Institute of Aeronautical Materials: Aero Engine Corporation of China Beijing Institute of Aeronautical Materials

**Hua-Ping Xiong**
xionghuaping69@sina.cn

Beijing Institute of Aeronautical Materials

**Bo-xuan Zhao**
AVCC Beijing Institute of Aeronautical Materials: Aero Engine Corporation of China Beijing Institute of Aeronautical Materials

**Si-si Li**
AVCC Beijing Institute of Aeronautical Materials: Aero Engine Corporation of China Beijing Institute of Aeronautical Materials

**Jia-yu Qiu**
AVCC Beijing Institute of Aeronautical Materials: Aero Engine Corporation of China Beijing Institute of Aeronautical Materials

**Xin-yu Ren**
AVCC Beijing Institute of Aeronautical Materials: Aero Engine Corporation of China Beijing Institute of Aeronautical Materials

---

**Research Article**

**Keywords:** DD6 single-crystal superalloy, vacuum brazing, CoNiCr-B based filler metal, strengthening alloying elements, microstructure

**Posted Date:** November 6th, 2026

**DOI:** https://doi.org/10.21203/rs.3.rs-11310456/v1

**License:** This work is licensed under a Creative Commons Attribution 4.0 International License.
Read Full License

# Abstract

Series of CoNiCr based filler metals were designed for vacuum brazing single crystal superalloyDD6. The influences of strengthening elements (W, Mo, Nb) in CoNiCr-B based filler metal on joint microstructure and boride formation were investigated using SEM and EDS. The results reveal that W, Mo and Nb participate in boride formation within the brazing seam. As the strengthening-element content increase, the boride morphology was changed from discrete vein-like dendrite to blocky, acicular of fragmented brittle phases. Excessive addition of the strengthening element leads to coarse aggregregated borides, which act as potential crack-initiation sites. Molybdenum exerts the strongest morphological modification effect, producing acicular borides at high content. High-Nb addition yields fragmented blocky borides. Tungsten mainly enlarges original vein-like boride dimension before destroying dendritic features. This work provides fundamental support for composition optimization of brazing fillers for single crystal superalloy components.


# 1 Introduction

Ni-based alloys are widely used in the aeronautics industry for their excellent high-temperature strength and corrosion resistance[1, 2]. As the most important aeronautic component, the turbine blades endure extreme high-temperature load and multi-axial complex stress during service. Single crystal superalloy DD6 developed in China has high-temperature strength, microstructure stability and casting performance. Consequently, DD6 is extensively adopted for manufacturing air-cooled turbine blades in the field of aeroengines[3, 4].

Advanced turbine blades generally contain intricate internal cooling cavities, and joining technologies are therefore indispensable for blade manufacturing[5, 6]. Conventional fusion welding encounters obvious limitations for superalloy castings, since high Al and Ti contents render these alloys susceptible to hot cracking[7]. For this reason, vacuum brazing using low-melting-point filler alloys is widely adopted for such applications[8]. In recent years, many studies focused on the brazing of Ni-based single crystal superalloy. Laux B etal.[9, 10] brazed single crystal superalloy N5 using Ni-Mn-Cr-Al-Ti filler alloy and good metallurgical bonding was obtained. Broomfield R W[11] attempted to braze CMSX-4 single-crystal superalloy with various Ni-based fillers, yet grain boundaries within joints weakened. Sun Y[12] designed Co-Ni-Cr-W-Si-B filler alloy to braze the single crystal superalloy DD5, andthe results showed that the coarse borides would weaken the joint strength. In previous work[13], our research group designed Ni-Cr-Co-Pd-W-Al-Ti-Mo-B complex filler alloy, the matrix of brazing seam was composed of γ＋γ' dual phase which was similar to the DD6 base material. There are also many applications of high-entropy alloy interlayer were designed for brazing superalloys[14, 15]. A high-entropy alloy without Si and B named as Ni-Co-Cr-Al-Nb-Ti was proposed for the brazing of single crystal superalloy DD6, andfast epitaxial solidificationwas realized in the brazing seam[16].Although multiple filler systems have been explored for joining of singlecrystalsuperalloy, the strengthening mechanisms of different alloying elements in brazed joints remain unsystematically investigated.

In this study, typical strengthening elements in superalloy system, namely W, Mo and Nb, were incorporated into CoNiCr-Bbased filler alloys. The effects of element and addition content on joint microstructure and mechanical performance were systematically evaluated.

# 2 Experimental procedures

The base material was the secondgeneration singlecrystal superalloy DD6 which was developed in China. Long strip test panel with the size of 130×38×27 $mm^3$ were prepared by industrial directional solidification furnace. Then the specimens were subjected to the following solution treatment (i.e. 1290˚C/1 h + 1300˚C/2 h + 1315˚C/4 h/air cooling) and aging treatment (i.e. 1120◦C/4 h/air cooling + 870◦C/32 h/ air cooling). Nominal chemical composition and tensile properties at 980°C are summarized in Table 1[17]. The typical microstructure of fully heat-treated single crystal superalloyDD6 is shown in Fig. 1.

Table 1
Chemical composition (wt.%) and tensile properties of singlecrystal superalloyDD6 tested at 980°C

| Cr | Co | W | Mo | Al | $\sigma_b$/ | $\sigma_{p0.2}$/ | δ/% | ψ/ % |
|---|---|---|---|---|---|---|---|---|
| 3.8–4.8 | 8.5–9.5 | 7.0–9.0 | 1.5–2.5 | 5.2–6.2 | MPa | MPa | | |
| Nb | Ta | Re | Hf | Ni | 800 | 680 | 27.0 | 34.0 |
| 0.6–1.2 | 6.0-8.5 | 1.6–2.4 | 0.05–0.15 | Bal. | | | | |

(60Co-20Ni-20Cr)-*X*-3B series filler alloys were designed, in which X refers to element W, Moand Nb. In every kind of alloy, the mass percentage of *X* was set as 4%, 8%, 12% and 16%. 3% element B was constantly added as melting-point depressant. (60Co-20Ni-20Cr)-3B filler alloy was also fabricated for comparison. The compositions of all 13-kind filler alloys were listed in Table 2. Filler alloys were manufactured as follows: high-purity Co, Ni, Cr, B, W, Mo and Nb raw metals were weighed according to target compositions; filler ingots were then fabricated via vacuum arc melting. Subsequently, ingots were sliced into 1 mm-thick foils.

Table 2
Nominal composition of designed filler alloys

| Number | Compositions (wt, %) | | | | | | |
|---|---|---|---|---|---|---|---|
| | Co | Ni | Cr | W | Mo | Nb | B |
| 1# | 58.2 | 19.4 | 19.4 | - | - | - | 3 |
| 2# | 55.8 | 18.6 | 18.6 | 4 | - | - | 3 |
| 3# | 53.4 | 17.8 | 17.8 | 8 | - | - | 3 |
| 4# | 51.0 | 17.0 | 17.0 | 12 | - | - | 3 |
| 5# | 48.6 | 16.2 | 16.2 | 16 | - | - | 3 |
| 6# | 55.8 | 18.6 | 18.6 | - | 4 | - | 3 |
| 7# | 53.4 | 17.8 | 17.8 | - | 8 | - | 3 |
| 8# | 51.0 | 17.0 | 17.0 | - | 12 | - | 3 |
| 9# | 48.6 | 16.2 | 16.2 | - | 16 | - | 3 |
| 10# | 55.8 | 18.6 | 18.6 | - | - | 4 | 3 |
| 11# | 53.4 | 17.8 | 17.8 | - | - | 8 | 3 |
| 12# | 51.0 | 17.0 | 17.0 | - | - | 12 | 3 |
| 13# | 48.6 | 16.2 | 16.2 | - | - | 16 | 3 |

DD6 basealloy specimens were machined to dimensions of 24 mm × 14 mm × 2 mm. Brazing assemblies were prepared with a 100 μmparallel gap perpendicular to the [001] crystallographic direction of DD6. Vacuum brazing was performed at 1220°C for 15 min under vacuum maintained between $1.5 \times 10^{-3}$ Pa and $6.5 \times 10^{-3}$ Pa.

Crosssections of brazed joints were characterized by scanning electron microscopy (SEM) coupled with energy-dispersive X-ray spectroscopy (EDS). Quantitative elemental analysis was implemented using an electron probe microanalyser (EPMA, JXA-8100). High-temperature tensile tests of brazed joints were conducted at 980°C using specimens illustrated in Fig. 1(b). To clarify fracture mechanisms, fractured cross section and fracture surfaces were further examined by SEM.

# 3 Results and discussion

## 3.1 Microstructure and formation mechanism of joint brazed with CoNiCr-3B based filler alloy

Fig. 2 shows the joint microstructure of DD6 brazed withCoNiCr-3B filler alloy. No obvious cracks are observed within joint regions, confirming adequate filler wettability and sound metallurgical bonding. The

joint contains three typical microzones: diffusion-affected zone (Zone I, DAZ), isothermally-solidified zone (Zone II, ISZ) and athermally-solidified zone (Zone III, ASZ).

In Zone I, abundant brightwhite phases with blocky and acicular morphologies distributed between the DD6 base material and the braze alloy. Zone IIrepresentsa uniform grey matrix. We can find that elements Co, Ni and Cr are enriched here, according to the elemental area distribution maps in Fig.2. It could be derived from the CoNiCr-3B filler alloy. Zone III is a multi-phase mixed zone. The white fish-bone-like phase is enriched in W, Mo, Nb and B and corresponds to boride phases. Another dark-grey precipitate enriched in Cr and B is identified as Cr-rich boride. Both borides constitute eutectic constituents, and the complementary eutectic matrix phase located between borides shares identical chemical composition with Zone II. It should be noted that lightgrey domains within Zone III also possess compositions consistent with Zone II despite differences in image contrast.

To further interpret joint-formation behavior, etched joint microstructures are shown in Fig. 3, and EPMA quantitative results for representative microzones are summarised in Table 3. Microzone “1” lies at the interface between DD6 and the CoNiCr-3B filler alloy, with atomic-percent composition approximately 17.94% Ni, 14.65% Co, 8.36% W and 47.53% B. High W content yields high-contrast bright features under SEM. Meanwhile, boron exhibits extremely low solubility in nickel (0.3 at.% within 1060–1120 °C). Accordingly, these bright particles are primarily brittle Ni-Co-W-rich borides. Similar boride formation has been reported during brazing of 422 stainless steel with BNi-3 braze alloy[18,19].

**Table 3**EPMA analysis for typical microzonesmarked in Fig.3

| Micro zones | Atomic proportion (at%) | | | | | | | | | | Deduced phase |
|---|---|---|---|---|---|---|---|---|---|---|---|
| | Al | Cr | Co | Ni | Nb | Mo | Hf | W | Re | B | |
| 1 | 1.66 | 3.99 | 14.65 | 17.94 | 1.30 | 3.65 | / | 8.36 | 0.92 | 47.53 | Ni-Co-W-rich boride |
| 2 | 8.28 | 12.48 | 32.59 | 44.86 | 0.09 | 0.35 | / | 1.10 | 0.25 | / | Co-Ni-Cr |
| 3 | 7.66 | 13.66 | 33.85 | 43.36 | 0.07 | 0.30 | / | 0.89 | 0.21 | / | Co-Ni-Cr |
| 4 | 0.01 | 42.28 | 9.85 | 2.55 | 0.03 | 0.61 | / | 0.73 | 0.88 | 43.06 | CrB |
| 5 | / | 14.27 | 22.44 | 9.22 | 0.85 | 3.69 | / | 7.62 | 0.91 | 40.95 | Co-Ni-Cr, W-Mo-Nb-rich borides |
| 6 | 0.46 | 17.16 | 32.83 | 42.98 | 0.10 | 0.07 | 0.02 | 0.18 | / | 6.20 | B enriched in the Co-Ni-Cr grain boundary |

The matrix microzone “2” consists mainly of 44.86 % Ni, 32.59 % Co and 12.48 % Cr, with negligible boron; microzone “3” shows nearly identical composition. Fig. 3(c) reveals diverse grain-orientation features. Our earlier work[12] reported analogous Co-Cr-rich matrix phases for Co-based brazing fillers. During isothermal holding at brazing temperature, Co-Ni-Cr phases nucleate and grow within liquid filler both at the DD6 substrate interface and at the central part of the joint. As Co-Ni-Cr grains propagate, solid-liquid interfaces advance outward. After solidification, compositional segregation of Co, Ni and Cr takes place because of their relatively slow diffusion kinetics and insufficient homogenization [12,20].

Upon completion of brazing isothermal holding, residual liquid phase possesses high boron concentration. During cooling, low-melting-point eutectic reactions proceed, generating boride phases at joint centers such as microzone “4” and “5” . According to elemental mapping (Fig. 2), microzone “4” is enriched in Cr and B, with Cr/B atomic ratio close to 1:1, confirming CrBintermetallics. Ohsasa et al[21] simulated residual-liquid-phase solidification for Ni-B-Cr ternary filler-metal TLP bonding; their results indicated full solidification at 997 °C via eutectic reaction: $L \rightarrow FCC_{\gamma}+Ni_3B+CrB$. Microzone “5” is enriched in refractory strengthening elements W and Mo. Idowu et al[22] investigated TLP bonding of INCONEL 738L superalloy with Ni-Cr-B-based fillers and observed Cr-Mo-W-B-rich intermetallics identified as $M_{23}B_6$ or $M_6B$ compounds. In addition, boron segregates to Co-Ni-Cr grain boundaries, as exemplified by microzone “4”.

## 3.2 The influence of the strengthening elements on joint microstructure

Adding strengthening elements to CoNiCr-3B based filler induces pronounced microstructural evolution within brazed joints. Fig. 4 presents joint cross-section micrographs for different strengthening-element concentrations. Different element types produce distinct boride morphologies. Increasing strengthening-element content raises the volume fraction of boride phases within seams. At 4 wt.% addition, boride fraction exhibits little difference compared with the CoNiCr-3B filler alloy.

For W-modified CoNiCr-3B fillers, tungsten preferentially partitions into white boride phases inside brazing seams. Increasing W content increases the volume fraction of fishbone-like borides, while the overall morphology remains largely unchanged.

For CoNiCr-Mo-3B systems, Mo reacts with boron to form borides. Raising Mo content drastically increases boride volume fraction. At 12 wt.% Mo, fishbone-like borides distribute uniformly across the entire brazing seam. At 16 wt.% Mo, borides transform from fishbone-like to acicular morphology.

When Nb is individually added to CoNiCr-3B, continuously distributed serrated grey phases form at joint centers, with white boride particles embedded within these grey phases or along serrated phase boundaries. Increasing Nb content elevates boride fraction and expands their distribution range. At 16 wt.%Nb, borides become homogeneously dispersed throughout the whole brazing seam.

## 3.3 The influence ofstrengthening elements on joint tensile strength

High-temperature tensile performance of brazed DD6 joints was characterized at 980 °C; test results are plotted in Fig. 5. Joints produced with CoNiCr-3B based filler exhibit extremely low strength and fractured prior to formal tensile loading, owing to the absence of W, Mo and Nb strengtheners.Upon W addition, joint strength rises with increasing W content, although the strengthening rate slows above 12 wt.% W. For Mo-containing fillers, joint strength increases-decreases-increases with rising Mo content and achieves maximum strength at 16 wt.% Mo. Nb also delivers remarkable strengthening; nevertheless, joint strength drops sharply at 16 wt.% Nb, and specimens fracture before tensile testing. Overall, appropriately-added Mo and Nb provide superior joint-strengthening effects compared with W. Therefore, future filler-metal design may adopt reduced W content coupled with optimized Mo and Nb additions.

Fig. 6 shows cross-section fracture profiles for joints with 12 wt.% W, Mo and Nb additions. All fractures propagate through the central brazing-seam region, indicating boride-rich zones constitute mechanical weak sites for crack initiation. Brittle boride phases deteriorate mechanical properties and environmental resistance of brazed joints[23], consistent with our earlier findings[13].

Further fracture-surface observations are shown in Fig. 7. Joints brazed with W-bearing fillers display relatively flat fracture surfaces, which contributes to inferior mechanical performance. By contrast, Mo- and Nb-modified joints exhibit rougher fracture topography and more tortuous crack-propagation paths, which favors enhanced mechanical performance. This explains why Mo- and Nb-containing joints achieve higher tensile strength compared with W-modified counterparts.

# 4 Conclusions

1. The joint of singlecrystal superalloyDD6 brazed with CoNiCr-3B filler consist of a substrate-adjacent reaction layer, CoNiCr-rich braze-matrix zone, and fishbone-like boride-rich zone. Two major boride types are identified: CrB borides and W- Mo- Nb-rich borides. W, Mo and Nb within brazing seams originate from DD6 substrate diffusion into liquid filler during brazing.
2. Microstructure is evidently modified after adding W, Mo and Nb into CoNiCr-3B filler. Increasing strengthening-element content increases the fraction of white fishbone-like borides within seams; CrB phases are gradually replaced by W-Mo-Nb-rich borides. When element addition exceeds 12 wt. %, borides gradually transform from fishbone-like to strip-shaped morphologies.
3. CoNiCr-3B filler produces DD6 brazed joints with low tensile strength. Appropriate additions of W, Mo or Nb effectively improve joint strength. Among all tested formulations, CoNiCr-12Nb-3B filler delivers the most prominent strengthening effect; its brazed joint achieves an average tensile strength of 503 MPa at 980°C. The corresponding fracture surface displays obvious rugged topography and highly tortuous crack paths, which benefits joint-strength improvement.

# Declarations

**Data availability**

The Data in this research work can be made available upon request

**Authorship contribution statement**

Wen-wen Li: Writing–original draft, Visualization, Data curation, Investigation;

Bo Chen: Writing–review & editing, Conceptualization, Supervision, Methodology

Hua-ping-Xiong: Writing–review & editing, Conceptualization, Supervision, Methodology

Bo-xuan Zhao: Resources, Methodology

Si-si Li: Resources, Methodology

Jia-yu Qiu: Resources

Xin-yu Ren: Project administration, Funding acquisition

**Funding**

This research was supported by the National Natural Science Foundation of China under grant Nos.52201050.

**Conflict of interests**

The authors declare no competing interests.

# References

1. Barazandeh R, Mofid MA, Jafarzadegan et al (2023) Wide gap brazing of NIMONIC 105 superalloy using BNi-2 filler and the effect of post braze heat treatment on joint properties. Weld World 67:1325–1336
2. Liu JD, Jin T, Zhao NR et al (2011) Microstructural study of transient liquid phases bonded DD98 and K465 superalloys at high temperature. Mater Charact 62:545–553
3. Li J, Jin H, Liu S (2007) Stress rupture properties and microstructures of the second generation single crystal superalloy DD6 after long term aging at 980°C. Rare MetEng36(10):1784–1787
4. Shi Z, Li J, Liu S et al (2011) High cycle fatigue behavior of the second generation single crystal superalloy DD6. T Nonferr MetalSoc21:998–1003
5. Fernandez-Zelaia P, Kirka M, RossyAet al (2021) Nickel-based superalloy single crystals fabricated via electron beam melting. Acta Mater 216:117133–117131
6. Zhang Z, Liu J, Qiu K et al (2023) Effects of brazing temperature on microstructure and high-temperature strength of joints using a novel fourth-generation nickel-based single crystal superalloy. Met Mater Int 29(2):444–456

7. Henhoeffer T, Huang X, Yand S (2010) Microstructure and high temperature tensile properties of wide gap brazed cobalt based superalloy X-40. MaterSci Tech-Lond 26:431–439
8. Ren X, Wang H, Li W et al (2024) Effect of holding time on interfacial evolution and mechanical strength of wide-gap brazed K417G superalloy joints. Weld World 68(12):3079–3084
9. Laux B, Piegert S, Rösler J (2010) Advanced braze alloys for fast epitaxial high-temperature brazing of single-crystalline Nickel-base superalloys. JEngGas Turbines Power 132(3):032101–032101
10. Laux B, Piegert S, Rösler J (2009) Braze alloy development for fast epitaxial high-temperature brazing of single-crystalline Nickel-based superalloys. Metall MaterTransA 40A(1):138–149
11. Broomfield RW (2000) Development of brazing techniques for the joining of single crystal components. Proceedings of the 5th International Charles Parsons Turbine Conference, Cambridge: Cambridge University Press,pp741–754
12. Sun Y, Hou X, Jin T et al (2017) Microstructure and mechanical properties of DD5 single crystal superalloy brazing joint. Trans China Weld Inst 38:117–120 (In Chinese)
13. Li W, Chen B, Xiong H et al (2021) Microstructure and the Mechanical Property of the high-performance DD6 Superalloy. Joint ActaMetall Sin 57(8):959–966 (In Chinese)
14. Li H, Zhou X, Chen Y et al (2026) High-entropy alloy interlayer-mediated joining of dissimilar materials: a review. Weld World. https://doi.org/10.1007/s40194-026-02626-5
15. Zhai Z, Ren X, Ren H et al (2025) Dissimilar joining of TiAl alloy to Ni-based superalloy using a Ni-Co-Fe-Mn-Cr-Ge-(Si,B) high-entropy alloy as brazing filler metal. 70:2315–2327Weld World
16. Ren X, Li W, Xiong H et al (2024) Fast epitaxial brazing of DD6 single crystal superalloy using novel NiCoCrAlNbTi high entropy filler alloy. JAlloy Compd 985:174082–174081
17. Editor committee of Chinese handbook of aeronautical materials (2002) Chinese hand book of aeronautical materials: deforming superalloy and casting superalloy. Version 2.(In Chinese)
18. Mohammd AM, Reza B, Mostafa J (2023) Vacuum brazing of NIMONIC 105 superalloy using W-rich BNi-10 and conventional BNi-2 fillers. JOM 75:4749–4761
19. Ou CL, Shiue RK (2003) Microstructural evolution of brazing 422 stainless steel using the BNi-3 braze alloy. J Mater Sci 38:2337–2346
20. Cao J, Song X, Zheng Z et al (2011) Effect of diffusion time on interfacial microstructure of TLP joints of DD6 single superalloy. Trans China Weld Inst 7:13–16 (In Chines)
21. Ohsasa K, Narita T, Shinmura T (1999) Numerical modeling of the transient liquid phase bonding process of Ni using Ni-B-Cr ternary filler metal. Phase Equilib 20(3):199–206
22. Idowu OA, Ojo OA, Charturvedi MC (2006) Microstructure study of transient liquid phase bonded cast Inconel 738L superalloy. Metall MaterTransA 37A:2787–2796
23. Huang X, Miglietti W (2012) Wide gap braze repair of gas turbine blades and vanes-a review. JEngGas Turbines Power 134:010801–010801

# Figures

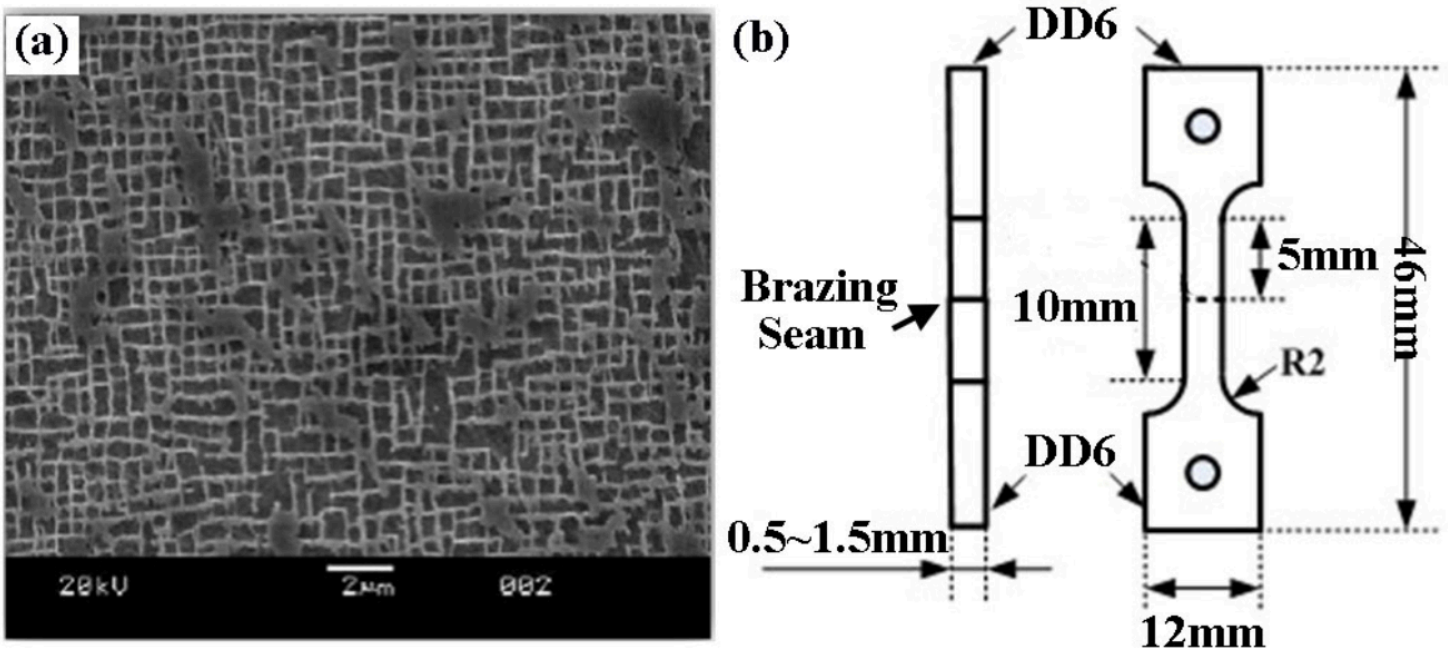



**Figure 1**

Typical microstructure of DD6 single crystal superalloy(a) and the schematic diagram of brazed joint for high-temperature tensile testing (b)

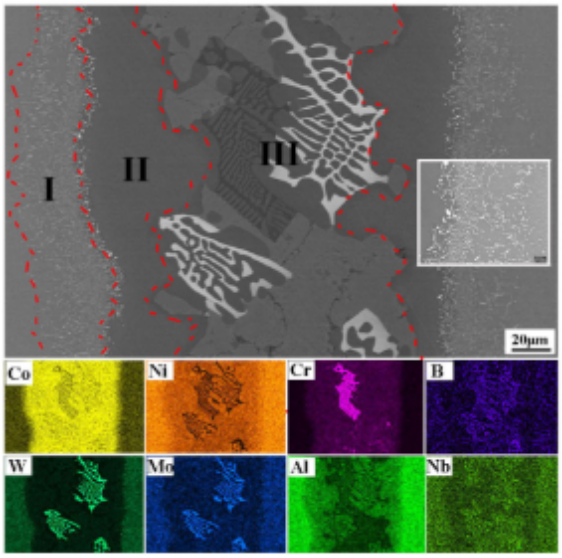



**Figure 2**

Microstructure and corresponding elemental distribution maps of the DD6 joint brazed with CoNiCr-3B filler alloy

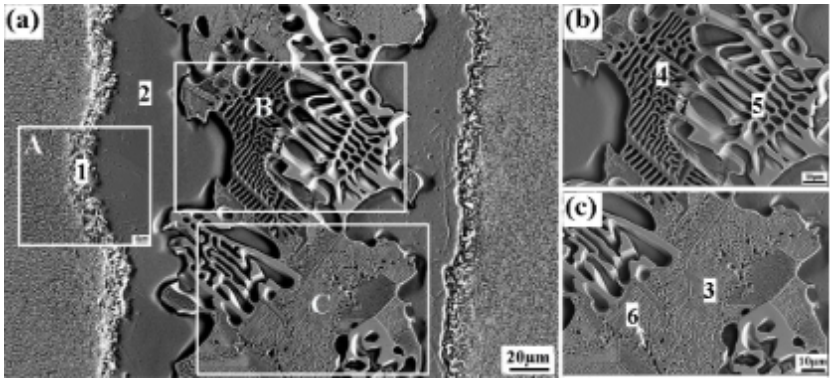



**Figure 3**

Microstructure of etched brazed joint: (a) overall joint morphology with magnified view of area A; (b) magnified micrograph of area B; (c) magnified micrograph of area C

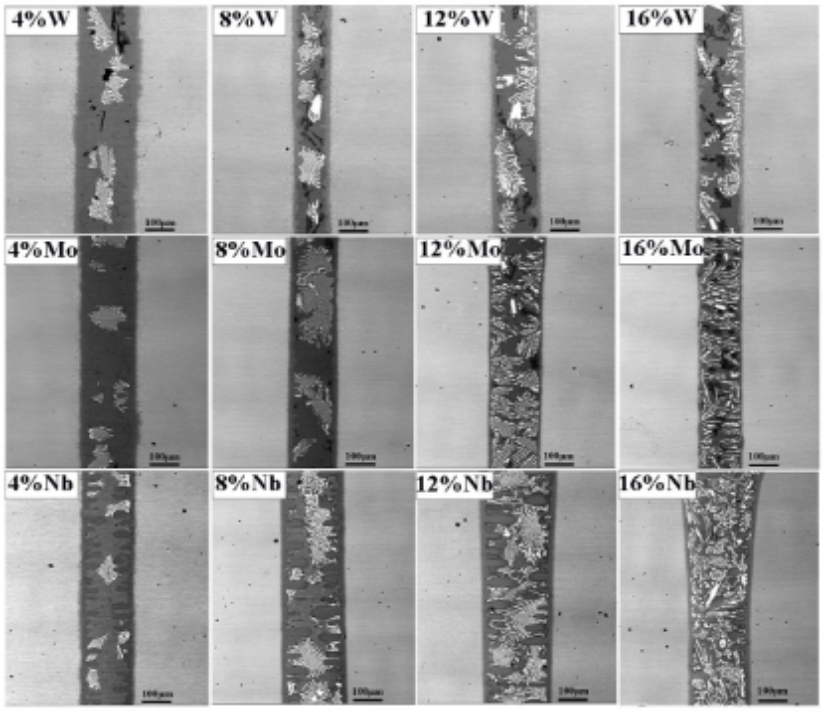



**Figure 4**

Microstructure of joints brazed with fillers containing different strengthening-elements content

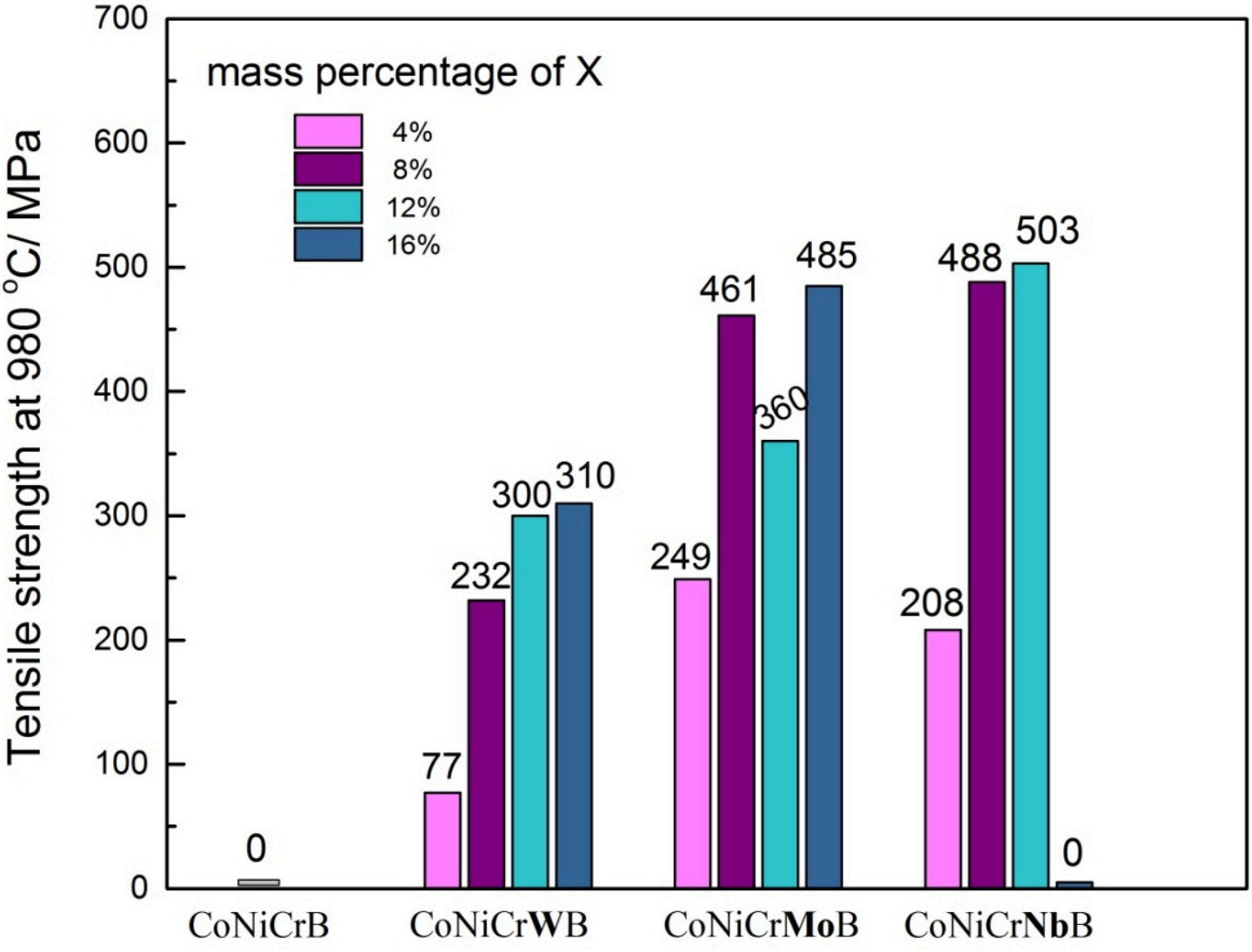



**Figure 5**

Tensile strength of the joints tested at 980 °C

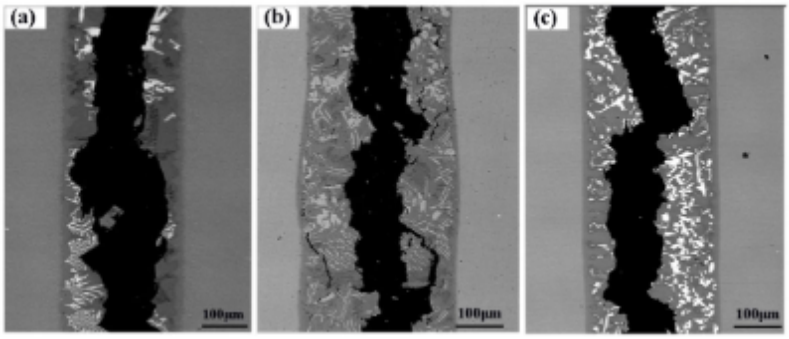



**Figure 6**

Fractured cross-section of the joints with different strengthening element:

(a)12% W, (b)12%Mo, (c)12%Nb

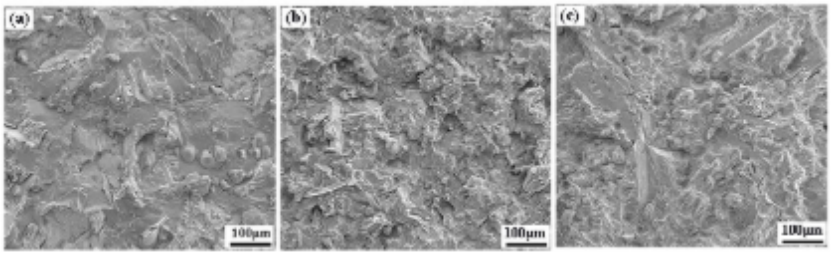



**Figure 7**

Fractured surface morphologies of joints with different strengthening element:

(a)12% W, (b)12%Mo, (c)12%Nb